Electron correlations in nonsequential double ionization of argon atoms by elliptically polarized laser pulses*

Yu Ben-Hai(余本海)†, Li Ying-Bin(李盈傧), and Tang Qing-Bin(汤清彬)

College of Physics and Electronic Engineering, Xinyang Normal University, Xinyang 464000, *China*

(Received 4 May 2012; revised manuscript received 21 June 2012)

Using a classical ensemble model, we investigate the correlation behaviour of electrons originating from nonsequential double ionization (NSDI) of argon atoms by the elliptically polarized laser pulses. Because of the ellipticity, not only the first electron to return but also the later return of tunneled electrons contribute significantly to NSDI. We mainly discuss two kinds of events of NSDI originating from the first and the second return separately. For the NSDI resulting from the recollision of the first return, the correlated electron momentum spectrum along the long axis of the laser polarization plane reveals an obvious V-like shape, located at the first and third quadrant. However, for the NSDI resulting from the recollision of the second return, the momenta of two electrons are distributed in the four quadrants uniformly. By analysing the trajectories of these two kinds, we find that the recollision energy and the laser phase at recollision are different for the first and second returning trajectories, which are responsible for the difference in the correlated behavior of the final electron momentum.

Keywords: nonsequential double ionization, elliptically polarized laser pulse, recollision, electron correlation

PACS: 32.80.Rm, 31.90.+s, 32.80.Fb **DOI:** 10.1088/1674-1056/22/1/013206

1. Introduction

Nonsequential double ionization (NSDI) of atoms and molecules in intense laser fields has become one of the central and most controversial topics in the past three decades, and has also induced a great number of experimental and theoretical studies,[1–13] because it reveals very high electron correlations. Recent experiments[5,7,9] have provided convicting evidence that the rescattering picture is the mechanism responsible for NSDI.[14] According to this model, the first electron is ionized via tunneling the Coulomb barrier which is tipped down by the laser electric field. Secondly, the electron is carried away and then driven back to the parent ion as the laser field reverses its phase. Thirdly, the energetic returning electron returns to the parent ion and kicks out the second electron.[15] This rescattering process is also responsible for high-order harmonic generation.[16–22]

According to the three-step recollision theory, there are few or no NSDI events when the laser field is elliptically polarized or circularly polarized because the tunneled electron cannot return to its parent ion. This picture was confirmed by previous experimental measurements.[23] However, it is inconsistent with the results of subsequent experiments. Characteristic NSDI events have been observed for the molecules NO, O_2,[24,25] and atomic magnesium[26] under circular polarization. On the basis of a semiclassical model, Shvetsov *et al.*[27] investigated various distributions of ion and electron momenta in NSDI by an elliptically polarized laser field, and they found that the main contribution to NSDI comes from longer orbits for the sufficiently large ellipticity. On the basis of a classical ensemble model, Wang and Eberly[28] have found that the degree of elliptical polarization in an intense short laser pulse is related to the timing of a strong-field NSDI, and the higher ellipticity pushes the initiation of double ionization (DI) into a narrower time window, and they also found that all of the successful NSDI events come from recollisions at the end of an elliptical trajectory.[15]

In the present paper, applying a classical ensemble model, we examine the correlation behavior of the electrons in the NSDI of argon atoms by 800-nm, 2.0×10^{14}-W/cm^2 elliptically polarized laser pulses. Because of the ellipticity, not only the first returning (FR) but also the later returning tunneled electrons contribute significantly to the NSDI. For the first returning trajectories (the recollision leads to DI occurring at the first returning), we find a V-like structure in the final-state momentum spectra of two electrons along the long axis of the laser polarization plane, which is because the tunneled electrons have higher recollision energy and NSDI occurs through recollision ionization (RCI).[29] For the SR trajectories (the recollision brings about DI at the second returning), the final-state momenta of two electrons along the long axis of the laser polarization plane are distributed in the four quadrants uniformly. This is because the recollision excitation with a subsequent ionization (RESI) mechanism dominates the NSDI.[29] We also analyse the microscopic dynamics of the

*Project supported by the National Natural Science Foundation of China (Grant Nos. 11005088 and 11047145), the Project of Basic and Advanced Technology of Henan Province, China (Grant Nos. 102300410241 and 112300410021), and the Scientific Research Foundation of Education Department of Henan Province, China (Grant No. 2011B140018).

†Corresponding author. E-mail: hnyubenhai@163.com

© 2013 Chinese Physical Society and IOP Publishing Ltd

later returns (LR) which correspond to the third, fourth, and subsequent returns of the tunneled electrons. In the direction of the short axis of the laser polarization plane, the final-state momentum distribution of Ar^{2+} ion for the FR trajectories is broader than that of the SR trajectories.

2. Classical ensemble model

The classical ensemble model was introduced in Ref. [30] and was successful in understanding the physical process of the NSDI.[31–34] Our classical ensemble contains 2.0×10^6 argon atoms. The ellipticity ε is set to be 0.1 because there are less NSDI from SR trajectories for $\varepsilon = 0$ (linear polarization laser pulse) and less NSDI from FR trajectories for $\varepsilon > 0.1$. In the classical model, the evolutions of the two electrons are governed by Newton's classical equations of motion[30,33] (atomic units are used throughout unless otherwise stated), which is expressed as

$$\mathrm{d}^2\boldsymbol{r}_i/\mathrm{d}t^2 = -\boldsymbol{\nabla}[V_{\mathrm{ne}}(\boldsymbol{r}_i) + V_{\mathrm{ee}}(\boldsymbol{r}_1,\boldsymbol{r}_2)] - \boldsymbol{E}(t), \tag{1}$$

where i is the electron label which runs from 1 to 2, $\boldsymbol{r}$ represents the two-dimensional (2D) space coordinate, and $\boldsymbol{E}(t)$ is the electric field of the laser pulse and is given by

$$\boldsymbol{E}(t) = \frac{E}{\sqrt{\varepsilon^2+1}}[\boldsymbol{e}_x\cos(\omega t) + \boldsymbol{e}_y\varepsilon\sin(\omega t)]f(t). \tag{2}$$

The laser field is elliptically polarized and has a trapezoidal pulse shape with two turn-on cycles, six cycles with full strength, and two turn-off cycles. The ε is the ellipticity, and ω is the laser frequency. The $\boldsymbol{e}_x$ represents the long axis of the laser polarization plane, and $\boldsymbol{e}_y$ represents the short axis of the laser polarization plane. The potentials are

$$\begin{aligned} V_{\mathrm{ne}}(\boldsymbol{r}_i) &= -2/\sqrt{\boldsymbol{r}_i^2 + a^2}, \\ V_{\mathrm{ee}}(\boldsymbol{r}_1,\boldsymbol{r}_2) &= 1/\sqrt{(\boldsymbol{r}_1-\boldsymbol{r}_2)^2 + b^2}, \end{aligned} \tag{3}$$

which represent the ion–electron and electron–electron interactions, respectively. In the classical model, we employ the softening parameter a to prevent one electron from dropping into the Coulomb well and transferring enough energy to the second electron for it to escape from the atom.[35] For the ground-state energy of the argon atom, i.e., -1.59 a.u., a must be above 1.26. There is also an upper limit for a. In order to be able to place the two electrons into a classically allowed region with a total energy of -1.59 a.u., the softening parameter must satisfy $a < 1.63$.[35] In the present paper, the soft parameter a is set to be 1.5. The softening parameter b in the e–e interaction is included to avoid the mathematical singularity in our calculations. We set b=0.05. A higher value of b can reduce the DI yield because of the weaker recollision.[35] Hence, these two softening parameters can be chosen arbitrarily so that they can satisfy the above condition.

To obtain the initial value, the ensemble's population starts from a classically allowed position for the argon atom whose ground-state energy is -1.59 a.u. The initial position of one electron is set to be (0.85, 0), and the other is set to be $(-0.85, 0)$. The available kinetic energy is distributed between the two electrons randomly in momentum space.[30] Each electron is only given a radial velocity with random directions. Then the electrons are allowed to evolve for a sufficiently long time (100 a.u.) in the absence of a elliptically polarized laser field to obtain stable position and momentum distributions.[30] Then we turn on the elliptically polarized laser pulse. At this moment, both the Coulomb field and laser field govern the evolutions of the two electrons. When the laser field is turned off, we determine the DI if both electrons gain positive energies.[30]

3. Results and discussion

Figures 1(a) and 1(b) display the final-state momentum distributions of correlated electrons along the long axis of the laser polarization plane (x axis), and along the short axis of the laser polarization plane (y axis), respectively. The V-like shape has been observed in previous experiments.[36,37] For instance, at 4.5×10^{14} W/cm^2, Staudent *et al.*[36] investigated the momentum distribution of two electrons freed by the NSDI of helium, and found a figure-like (or V-like) structure in the longitudinal direction (along the direction of laser polarization). At a much higher intensity, 1.5×10^{15} W/cm^2, Rudenko *et al.*[37] observed a pronounced V-like shape from the correlated electron momentum distribution. In our results, we also observe a V-like structure located at the first and the third quadrants, as shown in Fig. 1(a). The asymmetric distribution in the first and the third quadrant results from the fact that part of the trajectories are doubly ionized during the turn-on stage of the laser pulses. In Fig. 1(b), correlated electron momenta along the y axis are mainly distributed in the second and fourth quadrants, which indicates that most of the correlated electrons are emitted into the opposite hemisphere in the final state due to the repulsive electron interaction along the y axis.[33]

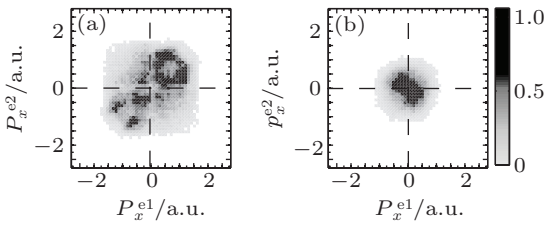


Fig. 1. Correlated electron momentum distributions for the NSDI of argon atoms in the directions along (a) the long axis, and (b) the short axis of the polarization plane.

In Figs. 2(a)–2(c), we separate the trajectories that are shown in Fig. 1(a) given that the recollisions lead to DIs at the

first return, the second return (SR), or the later returns (LRs), i.e., the third, fourth, and subsequent return of the tunneled electrons. For the FR trajectories, the correlated electron momenta along the x axis are mainly distributed in quadrants 1 and 3, and exhibit obvious V-like shapes, as shown in Fig. 2(a). For the SR trajectories, in the direction of the x axis, the momenta of the two electrons are distributed in the four quadrants uniformly, as shown in Fig. 2(b). For the LR trajectories, the V-like shapes still exist in quadrants 1 and 3 as shown in Fig. 2(c). In Figs. 2(d)–2(f), we present the number of DI trajectories versus the laser phase at recollision. Figures 2(d)–2(f) correspond to the trajectories shown in Figs. 2(a)–2(c), respectively. In Fig. 2(d), recollisions mainly occur just after the extremum of the field. However, in Figs. 2(e) and 2(f), recollisions mainly occur around zero crossing of the laser field. In order to understand the results shown in Figs. 2(a)–2(c), we display the energy distributions for the FR, SR, and LR trajectories (see Fig. 3). The time delays between the recollision and the DI are shown in Fig. 4 for the FR and SR trajectories.

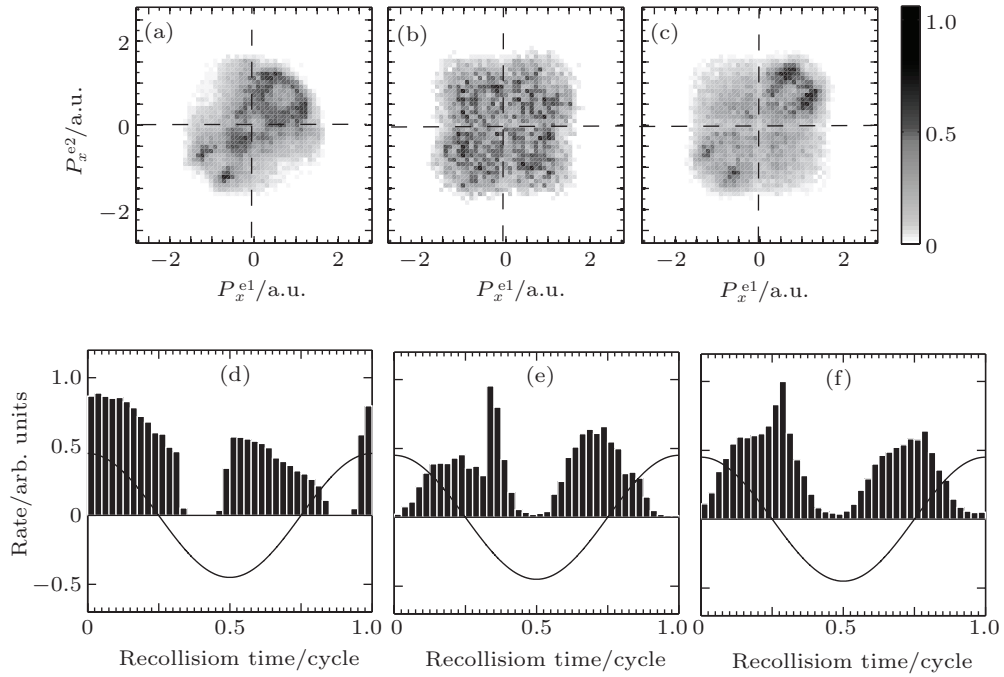


Fig. 2. Correlated electron momentum distributions along the x axis for the trajectories corresponding to the (a) FR, (b) SR, and (c) LR. (d)–(f): NSDI rates versus laser phase at recollision for the events given by (a), (b), and (c), respectively. The solid black curves represent laser fields along the x axis.

According to the simple-man model,[14] the electron with a much higher recollision energy returns to the parent ion near the zero crossing of the laser field. However, this picture is contrary to our result, i.e., the electrons which return to their parent ions near the extremum of the laser field possess a much higher recollision energy (see Fig. 3). This is because the recollision energy values of the FR trajectories are much higher than those of the SR trajectories, though the recollisions collectively occur just after the extremum of the field. Here, the recollision time is defined as the instant of the closest approach after the first departure of one of the two electrons.[33,34] The DI time is defined as the instant when both electrons achieve positive energies for the first time after recollision.[33,34] The recollision energy E_{e1} is defined as the kinetic energy $(v_x^2/2 + v_y^2/2$, where v_x and v_y represent the velocities of the returning electron) just before recollision.

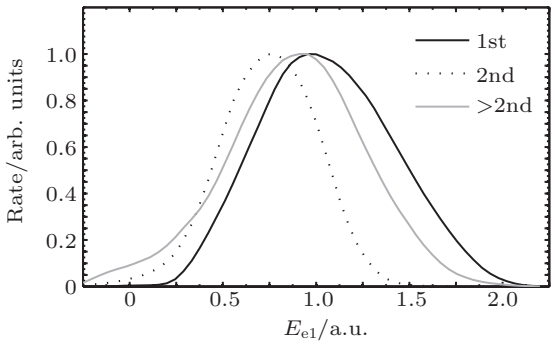


Fig. 3. The recollision energy distributions of the FR trajectories, SR trajectories, and LR trajectories.

In order to explore the responsible dynamics for the V-like shape in Fig. 2(a), we analyze the process of the NSDI. The final-state velocities of electrons along the x axis can be approximately described as[15]

$$V'_{x_i} = V_{0x_i} - \frac{1}{\omega} E \sin(\omega t_{0i}), \tag{4}$$

where ω is the frequency of the laser field, V_{0x_i} represents the initial velocity along the x axis at emission after recollision, and t_{0i} is the ionization time. It is clearly seen from Fig. 4 that for the FR trajectories, most of the time delays are located at $0.128T$ (T is the laser cycle), which shows that two electrons will be ionized almost simultaneously after recollision.[29] This indicates that the RCI mechanism dominates the NSDI. Thus, most of the correlated electrons are emitted into the same hemisphere and the final-state momenta are mainly distributed in the first and third quadrants (see Fig. 2(a)).[29] Hence, in Eq. (4), the second term on the right-hand side is the laser-induced drift velocity, which is approximately equal for the two electrons. The final-state velocities (V'_{x_i}) are determined by the initial velocities (V_{0x_i}). Therefore, it is easy to understand the V-like structure in Fig. 2(a). For the high recollision energy (the solid black curve in Fig. 3), the recollision electron passes through the parent ion very quickly. Thus, the time of the e–e interaction is so short that the recolliding electron can transfer only a small part of its energy to the bound electron, resulting in serious asymmetry for the initial velocity.[38] As a result, the final-state velocities of two electrons are asymmetric, resulting in V-like shapes in the first and third quadrants.

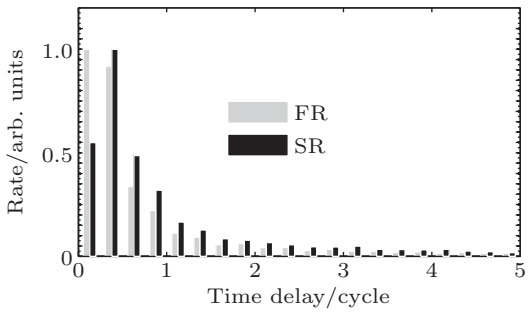


Fig. 4. Rate versus time delay between the recollision and DI for the FR trajectories and the SR trajectories.

At a relatively low laser intensity, theoretical studies have demonstrated that the final-state electron repulsion[2] contributes to the V-like shape. In order to examine whether the final-state electron repulsion is responsible for microscopic dynamics in our result (see Fig. 2(a)), we calculate the final-state momenta of two electrons in the case of excluding the e–e interaction from $0.06T$ after recollision. In other words, two electrons are allowed to evolve only under the nuclear Coulomb and laser field. Figure 5 shows the final-state momentum distribution of two electrons, the V-like shape is visible but is more obscure than that in Fig. 2(a). Thus, our result confirms that the electron repulsion also contributes to the V-like shape.

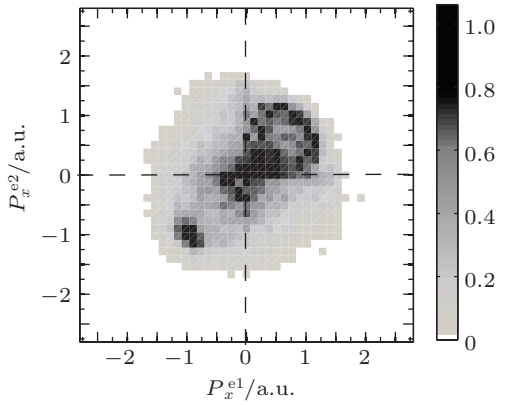


Fig. 5. Correlated electron momentum distribution along the x axis for the FR trajectories. Two electrons are allowed to evolve in the case of excluding the e–e interaction from $0.06T$ after recollision.

From the above analysis, we know that both asymmetric energy sharing (AES)[38] and the electron repulsion contribute to the V-like shape. The two facts are also responsible for the LR trajectories, as shown in Fig. 2(c). For the SR trajectories, most of the time delays are located at about $0.378T$, as shown by the black columns of Fig. 4. This indicates that the RESI mechanism dominates the NSDI. Thus, the final-state momentum of the correlated electron will be distributed in the four quadrants uniformly (see Fig. 2(b)).[29]

Finally, we display two sample trajectories in Fig. 6. Figure 6(a) shows that two electrons are ionized almost simultaneously after recollision, and emitted into the same hemisphere in the final state (see Fig. 6(c)). For the SR trajectories shown in the right column, one electron (the gray curve in Fig. 6(b)) is ionized before the first maximum of the field after recollision, while the other electron (the black curve in Fig. 6(b)) is ionized before the fourth maximum of the field. They are emitted into opposite hemispheres in the final state, as shown in Fig. 6(d). These results are consistent with that in Ref. [39]. For the FR trajectories, one electron will achieve a much higher velocity along the y axis in a final state than the other electron (see Fig. 6(e)). This is because the electron possesses a much higher energy after recollision, leading to a higher velocity in the direction of the y axis. However, for the SR trajectories, two electrons will achieve much lower or even close-to-zero velocities of the final state in the direction of the y axis (see Fig. 6(f)), as a result of much lower energy after recollision. Hence, the final-state momentum distribution of the Ar^{2+} ion along the y axis is much broader for the FR trajectories, as shown in Fig. 7.

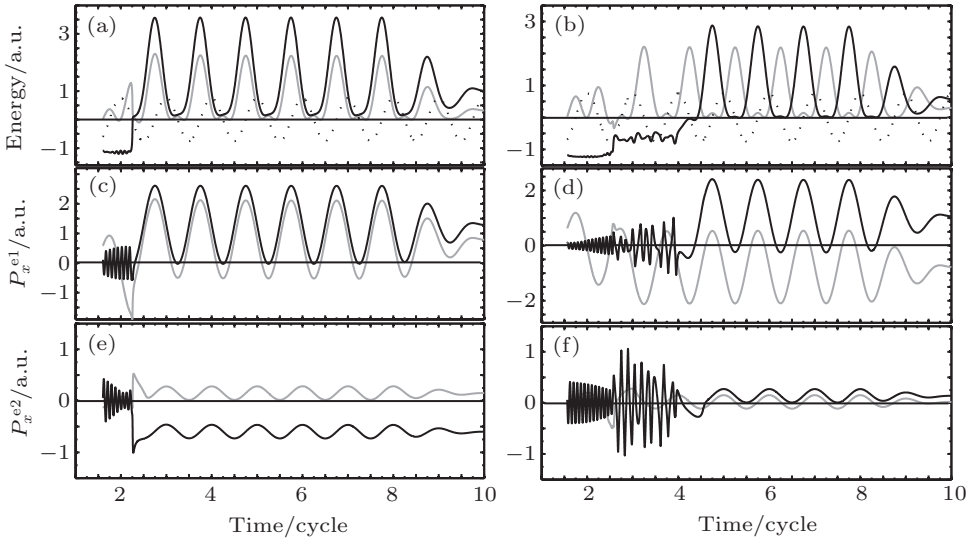


Fig. 6. Two sample trajectories selected from Fig. 2(a) (left column) and Fig. 2(b) (right column), respectively. (a), (b) Energy versus time; (c), (d) momentum of one electron along the x axis versus time; (e), (f): momentum of the other electron along the y axis versus time. The black dashed curves in (a) and (b) represent the laser fields along the x axis.

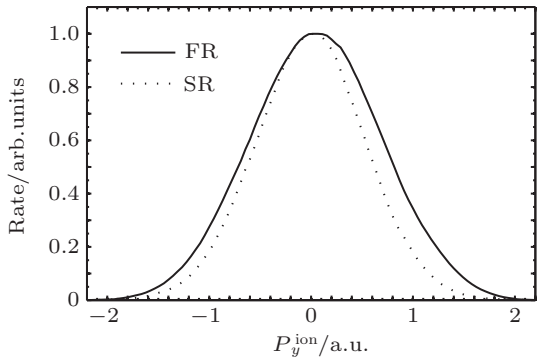


Fig. 7. Ar^{2+} ion momentum spectra along the y axis for the trajectories in Figs. 2(a) and 2(b), respectively. The solid curve represents FR; the dotted curve represents SR.

4. Conclusion

In this paper, we investigate the electron correlations in NSDI of argon atoms by the elliptically polarized laser pulses with a classical ensemble model. We mainly discuss the trajectories of NSDI from FR, SR, and LR trajectories. For the FR trajectories, the RCI mechanism dominates the NSDI and the momentum distributions of the correlated electron along the x axis and show obvious V-like structures in quadrants 1 and 3. Both electron repulsion and AES contribute to the V-like shape, and are also responsible for the LR trajectories. For the SR trajectories, the RESI mechanism dominates the NSDI, and the momenta of the two electrons along the x axis are distributed in the four quadrants uniformly. In addition, the final-state momentum distribution of the Ar^{2+} ion along the y axis is much broader for the FR trajectories because of the relatively high recollision energy.

References

[1] Zhou Y M, Liao Q and Lu P X 2010 *Opt. Express* **18** 16025
[2] Ye D F, Liu X and Liu J 2008 *Phys. Rev. Lett.* **101** 233003
[3] Liu Y Q, Tschuch S, Rudenko A, Dürr M, Siegel M, Morgner U, Moshammer R and Ullrich J 2008 *Phys. Rev. Lett.* **101** 053001
[4] Liao Q, Zhou Y M, Huang C and Lu P X 2012 *New J. Phys.* **14** 013001
[5] Weber T, Giessen H, Weckenbrock M, Urbasch G, Staudte A, Spielberger L, Jagutzki O, Mergel V, Vollmer M and Dorner R 2000 *Nature* **405** 658
[6] Zhou Y M, Liao Q, Zhang Q B, Hong W Y and Lu P X 2010 *Opt. Express* **18** 632
[7] Rudenko A, Zrost K, Feuerstein B, de Jesus V L B, Schröter C D, Moshammer R and Ullrich J 2004 *Phys. Rev. Lett.* **93** 253001
[8] Zhou Y M, Huang C, Liao Q, Hong W Y and Lu P X 2011 *Opt. Lett.* **36** 2758
[9] Weckenbrock M, Zeidler D, Staudte A, Weber Th, Schröter M, Meckel M, Kammer S, Smolarski M, Jagutzki O, Bhardwaj V R, Rayner D M, Villeneuve D M, Corkum P B and DÄorner R 2004 *Phys. Rev. Lett.* **92** 213002
[10] Zhou Y M, Huang C, Liao Q and Lu P X 2012 *Phys. Rev. Lett.* **109** 053004
[11] Huang C, Zhou Y M, Tong A H, Liao Q, Hong W Y and Lu P X 2011 *Opt. Express* **19** 5627
[12] Zhou Y M, Liao Q, Lan P F and Lu P X 2008 *Chin. Phys. Lett.* **25** 3950
[13] Liu X and Figueira de Morisson Faria C 2004 *Phys. Rev. Lett.* **92** 133006
[14] Corkum P B 1993 *Phys. Rev. Lett.* **71** 1994
[15] Wang X and Eberly J H 2010 *New J. Phys.* **12** 093047
[16] Hong W Y, Lu P X, Lan P F, Zhang Q B and Wang X B 2009 *Opt. Express* **17** 5139
[17] Cao W, Lu P X, Lan P F, Wang X L and Yang G 2006 *Phys. Rev.* A **74** 063821
[18] Yu B H, Zhang D L and Tang Q B 2011 *Chin. Phys.* B **20** 083201
[19] Lan P F, Lu P X, Li F, Li Y H and Yang Z Y 2008 *Opt. Express* **16** 5868
[20] Zhang Q B, Lan P F, Hong W Y, Liao Q, Yang Z Y and Lu P X 2009 *Acta Phys. Sin.* **58** 4908 (in Chinese)
[21] Cao W, Lu P X, Lan P F, Wang X L and Li Y H 2007 *Phys. Rev.* A **75** 063423
[22] Wang S Y, Hong W Y, Zhang Q B, Li Q G and Lu P X 2010 *Chin. Phys.* B **19** 083203
[23] Dietrich P, Burnett N H, Ivanov M and Corkum P B 1994 *Phys. Rev.* A **50** R3585
[24] Guo C, Li M, Nibarger J P and Gibson G N 1998 *Phys. Rev.* A **58** R4271

[25] Guo C and Gibson G N 2001 *Phys. Rev.* A **63** 040701
[26] Gillen G D, Walker M A and van Woerkom L D 2001 *Phys. Rev.* A **64** 043413
[27] Shvetsov N I, Goreslavski S P, Popruzhenko S V and Becker W 2008 *Phys. Rev.* A **77** 063405
[28] Wang X and Eberly J H 2010 *Phys. Rev. Lett.* **105** 083001
[29] Feuerstein B, Moshammer R, Fischer D, Dorn A, Schröter C D, Deipenwisch J, Crespo Lopez-Urrutia J R, Höhr C, Neumayer P, Ullrich J, Rottke H, Trump C, Wittmann M, Korn G and Sandner W 2001 *Phys. Rev. Lett.* **87** 043003
[30] Haan S L, Breen L, Karim A and Eberly J H 2006 *Phys. Rev. Lett.* **97** 103008
[31] Zhou Y M, Liao Q and Lu P X 2009 *Phys. Rev.* A **80** 023412
[32] Liao Q, Lu P X, Zhang Q B, Hong W Y and Yang Z Y 2008 *J. Phys.* B **41** 125601
[33] Zhou Y M, Huang C and Lu P X 2011 *Phys. Rev.* A **84** 023405
[34] Zhou Y M, Huang C, Tong A H, Liao Q and Lu P X 2011 *Opt. Express* **19** 2301
[35] Haan S L, Smith Z S, Shomsky K N and Planttinga P W 2009 *J. Phys.* B **42** 134009
[36] Staudent A, Ruiz C, Schröter M, Schröter S, Zeidler D, Weber Th, Mechel M, Villeneuve D M, Corkum P B, Becker A and Dörner R 2007 *Phys. Rev. Lett.* **99** 263002
[37] Rudenko A, de Jesus V L B, Ergler T, Zrost K, Feuerstein B, Schröter C D, Moshammer R and Ullrich J 2007 *Phys. Rev. Lett.* **99** 263003
[38] Zhou Y M, Liao Q and Lu P X 2010 *Phys. Rev.* A **82** 053402
[39] Haan S L, Smith Z S, Shomsky K N and Plantinga P W 2008 *J. Phys.* B **41** 211002